Research Article

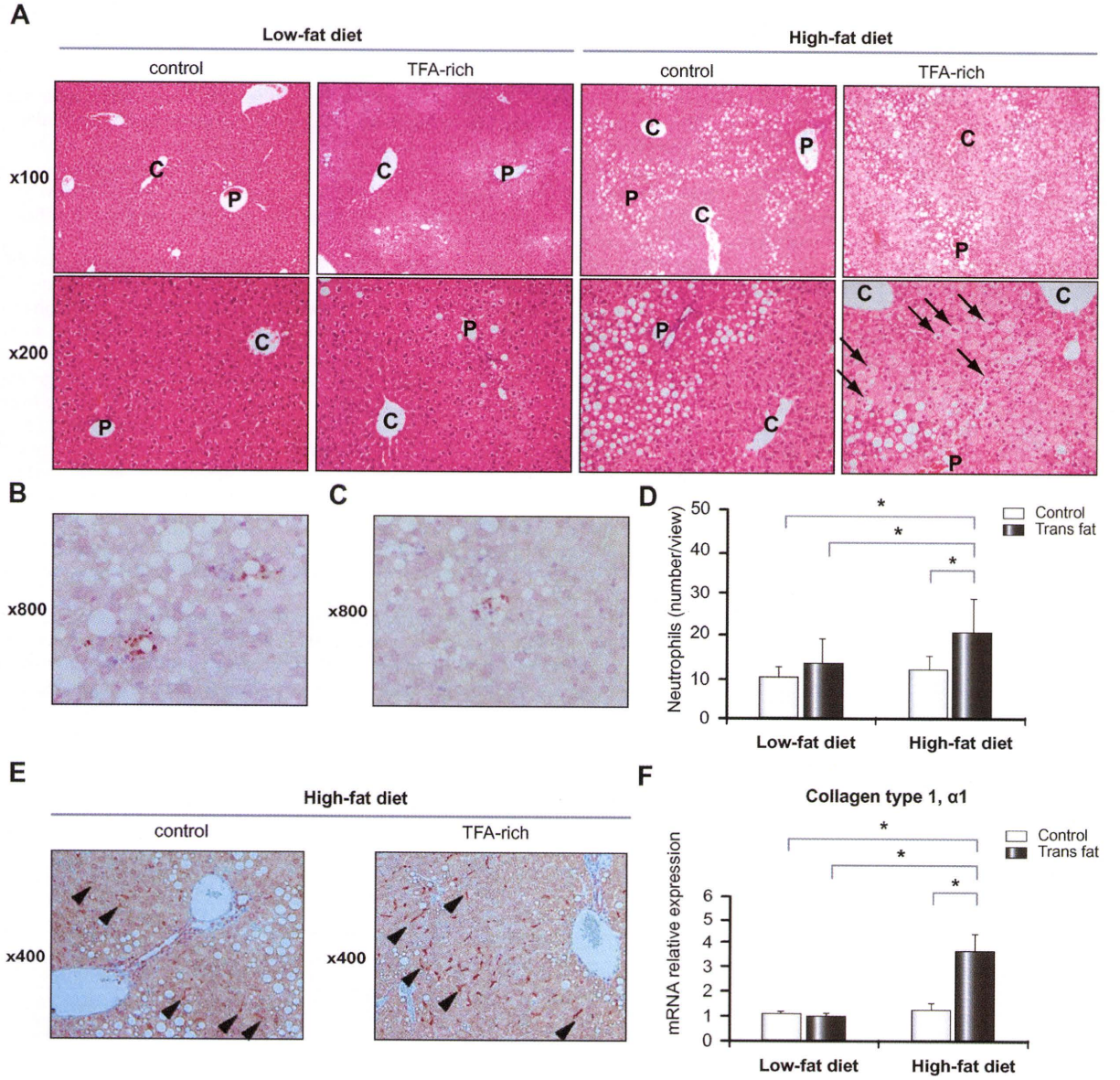

Fig. 1. Distinct steatotic features of the liver. (A) Representative liver histology stained with H&E. Remarkably expanded hepatocytes with extensive small lipid droplets make a feature of ballooning degeneration (arrows). Neutrophils confirmed by myeloperoxidase staining were (B) forming lipogranulomas and (C) surrounding the ballooning degenerated hepatocytes. (D) The number of neutrophils is increased in HF-T-fed mice liver. (E) KCs were detected by anti-F4/80 immunohistochemical staining (arrow heads). (F) Quantitative RT-PCR revealed elevation of collagen type 1, α1 mRNA expression in liver of HF-T-fed mice. P, portal tract; C, central vein. $^{*}p < 0.05$.

We evaluated the lipid composition of the liver to examine the pathological condition in the model. Compared to the LF-C group, the sum of total polyunsaturated fatty acid (PUFA), *n*-6 PUFA and *n*-3 PUFA was decreased in the LF-T group, but did not differ significantly in the other groups (Fig. 2E.). In the HF-C group, the sum of saturated fatty acid (SFA) and monounsaturated fatty acid (MUFA) was decreased, and total PUFA, *n*-6 PUFA and *n*-3 PUFA were increased compared to the LF-C group. However, in the HF-T group, total PUFA and *n*-6 PUFA decreased significantly compared to the LF-C group, and their proportions were similar to those of the LF-T group. The potentially beneficial lipid *n*-3 PUFA that is thought to prevent insulin resistance and hepatic steatosis [11], was increased even in the HF-T group compared to the LF-T group, the level of which was similar to that of the LF-C group.

The content of individual fatty acids in the liver coordinated nearly synergistically with the sum of the content of the fatty acids in the same unsaturation grade (Fig. 2E and Table 3). The unique accumulation of elaidic acid (18:1(9-*trans*)), chief component of dietary TFA, was noteworthy in the LF-T and HF-T groups. The content of arachidonic acid (20:4*n*-6) alone decreased to 70% only in the HF-T group, which was similar to the LF-T group in

Please cite this article in press as: Obara N et al. Possible involvement and the mechanisms of excess *trans*-fatty acid consumption in severe NAFLD in mice. J Hepatol (2010), doi:10.1016/j.jhep.2010.02.029

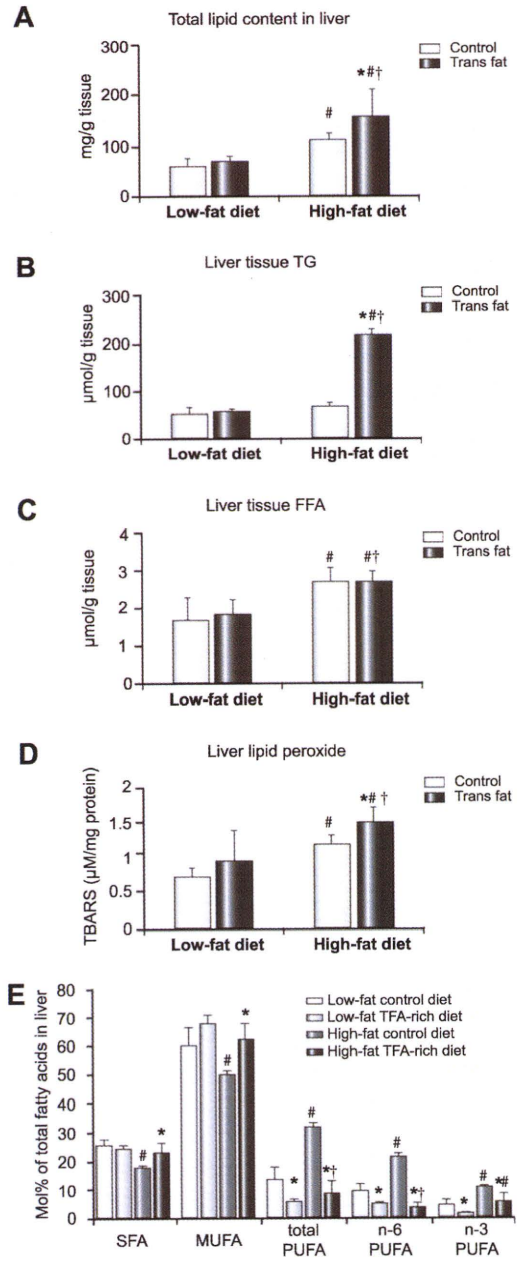

Fig. 2. Lipid accumulation in the liver. (A) Total lipid, (B) TG, and (C) FFA in the liver were measured and normalized to the tissue weight. (D) Lipid peroxide in the liver was measured and normalized by each amount of protein. (E) The hepatic fatty acid composition analyzed by gas chromatography was organized as follows: SFA, saturated fatty acid; MUFA, *cis*-monounsaturated fatty acid; PUFA, polyunsaturated fatty acid; *n*-6, *n*-6 PUFA; and *n*-3, *n*-3 PUFA ($n = 6$ for each group). *Significantly different from the control group with the same dietary composition; ‡significantly different from the low-fat diet with same dietary oil; † significantly different from LF-C-fed and HF-T-fed group.

terms of linoleic acid (18:2*n*-6), the precursor of arachidonic acid. Except for elaidic acid and arachidonic acid, there were no specific alterations for the HF-T group.

Cytokine-, adipokine- and lipid metabolism-related gene expression in liver

Real-time RCR showed that TNFα and inducible nitric oxide synthase (iNOS) mRNA expression increased in the HF groups compared to the LF groups by approximately 2-fold when evaluated for each C or T group (Table 4), while no difference was seen in IL-6 and transforming growth factor-β (TGF-β) mRNA expression in liver among all groups. In addition, adiponectin receptor 1 and 2 gene expression was measured as adipokine related genes, but they did not differ among all groups.

To examine the potential mechanisms of hepatic steatosis by the TFA-rich diet, we determined the expression of known mediators of lipogenesis, fatty acid oxidation and TG excretion in liver, the imbalance of which is thought to lead to steatosis. Sterol regulatory element-binding protein-1 (SREBP-1) induces fatty acid synthase (FAS) and acetyl CoA carboxylase (ACC), and is implicated in steatosis [27]. In relation to hepatic fatty acid synthesis, the mRNA expression of SREBP-1 was significantly elevated in the LF-T, HF-C and HF-T groups when compared to the LF-C group, whereas FAS and ACC were elevated significantly only in the HF-T group (Table 4). Peroxisome proliferator activated receptor γ (PPARγ) is also implicated in steatosis [33]. The expression of PPARγ1 did not differ among the groups, while PPARγ2 was significantly elevated 13-fold in the HF-C group and, remarkably, 50-fold in the HF-T group. Although, the expression of PPARγ coactivator-1β (PGC-1β), known to coactivate the SREBP-1 and stimulate lipogenic gene expression [19], was decreased in HF-fed mouse livers. The fatty acid oxidation-related genes of PPARα and carnitine palmitoyl transferase-1, and the TG excretion-related genes of microsomal triglyceride transfer protein and apolipoprotein B did not differ among the groups; fatty acid oxidation-related genes showed a tendency to be decreased in the LF-T group, but without statistical significance.

Concerning cholesterol metabolism-related gene expression in liver, SREBP-2 was increased in the HF groups, but was not affected by the dietary lipid sources. Hydroxymethylglutaryl-CoA synthase-1 and reductase were significantly increased and apolipoprotein A-1, a component of HDL, was decreased only in the HF-T group, while they did not change in the LF-T group, which showed an alteration of plasma cholesterol fraction (Table 4).

Phosphorylation status of AKT in high-fat diet-fed mice livers

As Koppe et al. suggested that TFA feeding increased insulin resistance in mice [17], and to determine if the exacerbating effects of TFA intake on liver were associated with increased insulin resistance, we evaluated the hepatic phosphorylation status of AKT (Fig. 3A). The phospho-AKT(Thr308) level was significantly decreased (Fig. 3B) and the phospho-AKT(Ser473) level was also decreased, but without statistical significance (Fig. 3C) as determined by densitometrical analysis.

TFA increases TNFα production and alters phagocytotic ability of KCs

The *cis*- or *trans*-fatty acid-containing medium showed no cytotoxicity towards KCs when compared to the fatty acid-free control medium (Fig. 4A). TNFα production of KCs induced by LPS was increased in both the C18:1 and C18:2 TFA-containing medium compared to that of *cis*-structural isomer-containing

Please cite this article in press as: Obara N et al. Possible involvement and the mechanisms of excess *trans*-fatty acid consumption in severe NAFLD in mice. J Hepatol (2010), doi:10.1016/j.jhep.2010.02.029

Research Article

Table 3. Individual fatty acid composition of the liver.

		Low-fat diet		High-fat diet	
		Control oil (LF-C)	TFA-rich oil (LF-T)	Control oil (HF-C)	TFA-rich oil (HF-T)
SFA					
Myristic	14:0	0.6 ± 0.1	0.5 ± 0.0	0.3 ± 0.1[‡]	0.4 ± 0.1[*†]
Palmitic	16:0	21.0 ± 1.6	19.2 ± 1.1	12.1 ± 0.6 [‡]	18.7 ± 3.6[*]
Stearic	18:0	3.7 ± 0.8	3.6 ± 0.6	4.6 ± 0.6	3.3 ± 1.2
Arachidic	20:0	0.6 ± 0.3	1.0 ± 0.1[*]	0.6 ± 0.3	0.9 ± 0.3
MUFA					
Palmitoleic	16:1 *n*-7	6.9 ± 4.9	7.9 ± 4.8	2.5 ± 0.2	4.9 ± 1.0
Oleic	18:1	53.4 ± 6.7	59.8 ± 2.3	47.4 ± 1.3	57.2 ± 4.8[*‡†]
Elaidic	18:1 (9-*trans*)	0.0 ± 0.0	2.2 ± 0.5[*]	0.3 ± 0.2	6.2 ± 2.4[*‡†]
PUFA					
Linoleic	18:2 *n*-6	6.5 ± 2.1	2.1 ± 0.4[*]	18.1 ± 1.6[‡]	2.6 ± 1.4[*†]
α-Linolenic	18:3 *n*-3	0.6 ± 0.4	0.0 ± 0.0[*]	3.2 ± 0.5[‡]	0.2 ± 0.2[*]
Dihomo-γ-linolenic	20:3 *n*-6	0.2 ± 0.1	0.2 ± 0.1	0.5 ± 0.2[‡]	0.2 ± 0.2
Arachidonic	20:4 *n*-6	2.5 ± 0.9	2.2 ± 0.5	2.6 ± 0.6	0.6 ± 0.3[*†]
Eicosapentaenoic	20:5 *n*-3	0.4 ± 0.2	0.1 ± 0.0	1.4 ± 0.1[‡]	1.2 ± 0.9[‡†]
Docosapentaenoic	22:5 *n*-3	0.2 ± 0.1	0.0 ± 0.0	0.8 ± 0.0[‡]	0.4 ± 0.3[*†]
Docosahexaenoic	22:6 *n*-3	3.0 ± 1.1	1.0 ± 0.3	5.2 ± 0.4	3.2 ± 2.4

The relative percentage (mean ± SD) of each fatty acid to the total fatty acids is presented ($n = 6$ per each group).
[*] Significantly different from the corresponding control group with the same dietary composition; $p < 0.05$.
[‡] Significantly different from the low-fat diet with the same dietary lipid as a source; $p < 0.05$.
[†] Significantly different from low-fat control diet group; $p < 0.05$.

medium (Fig. 4B). However, IL-6 production by KCs did not differ between *cis*- and *trans*-fatty acid-containing medium for both C18:1 and C18:2, respectively (Fig. 4C). The phagocytotic ability of KCs incubated in *trans*-C18:1-containing medium was lower than that in *cis*-C18:1-containing medium (Fig. 4D), while the influence of the structural difference of C18:2 fatty acid was small (Fig. 4E).

Discussion

Both of the dietary lipid species [3] and their amounts [6,23] are known to affect hepatic steatosis and inflammation. TFAs have been mainly linked with coronary heart disease, possibly by decreasing HDL-cholesterol and increasing LDL-cholesterol [20,29]; while little attention has been paid to liver disease, even

Table 4. Cytokine-, adipokine- and lipid metabolism-related gene expression in liver.

		Low-fat TFA-rich (LF-T)	High-fat control (HF-C)	High-fat TFA-rich (HF-T)
Cytokine and adipokine				
Tumor necrosis factor	TNF	0.98 ± 0.20	2.11 ± 0.73[‡]	1.94 ± 0.77[‡†]
Interleukin-6	IL-6	1.30 ± 0.28	1.16 ± 0.14	1.10 ± 0.25
Transforming growth factor-β	TGB-β	0.86 ± 0.17	1.35 ± 0.50	0.98 ± 0.22
Nitric oxide synthase 2, inducible	iNOS	1.29 ± 0.34	2.23 ± 0.75[‡]	2.69 ± 0.74[‡†]
Adiponectin receptor 1	AdipoR1	1.01 ± 0.17	1.29 ± 0.29	1.21 ± 0.25
Adiponectin receptor 2	AdipoR2	0.92 ± 0.16	1.20 ± 0.22	1.28 ± 0.26
Lipogenesis				
Fatty acid synthase	FAS	1.36 ± 0.21	0.79 ± 0.12	1.69 ± 0.46[*†]
Acetyl-CoA carboxylase	ACC	1.27 ± 0.10	0.80 ± 0.05	1.49 ± 0.37[*†]
Sterol regulatory element-binding protein-1	SREBP-1	3.76 ± 0.51[*]	1.93 ± 0.23[‡]	4.69 ± 0.17[*‡†]
Peroxisome proliferator activated receptor γ1	PPARγ1	1.45 ± 0.42	1.58 ± 0.48	1.29 ± 0.26
Peroxisome proliferator activated receptor γ2	PPARγ2	1.88 ± 0.33	12.92 ± 6.04[‡]	50.18 ± 3.61[*‡†]
PPARγ coactivator-1β	PGC-1β	0.81 ± 0.10	0.61 ± 0.15[‡]	0.59 ± 0.12[‡†]
Fatty acid oxidation				
Peroxisome proliferator activated receptor α	PPARα	0.51 ± 0.23	1.25 ± 0.48	1.28 ± 0.41
Carnitine palmitoyl transferase-1	CPT-1	0.63 ± 0.11	1.03 ± 0.34	1.08 ± 0.57
Triglyceride excretion				
Microsomal triglyceride transfer protein	MTP	1.04 ± 0.16	0.92 ± 0.11	0.91 ± 0.11
Apolipoprotein B	ApoB	1.11 ± 0.15	1.20 ± 0.13	1.15 ± 0.09
Cholesterol metabolism				
Sterol regulatory element-binding protein-2	SREBP-2	0.87 ± 0.15	1.66 ± 0.25	1.69 ± 0.34
Hydroxymethylglutaryl-CoA synthase-1	HMGCs1	1.03 ± 0.11	1.60 ± 0.26	4.56 ± 0.73[*‡†]
Hydroxymethylglutaryl-CoA reductase	HMGCr	0.99 ± 0.13	1.22 ± 0.32	2.93 ± 0.44[*‡†]
Apolipoprotein A-1	ApoA1	0.93 ± 0.09	1.26 ± 0.21	0.61 ± 0.11[*‡†]

All results are expressed as the relative fold change compared to the low-fat control diet group ± SD ($n = 6$ per each group).
[*] Significantly different from the corresponding control group with the same dietary composition; $p < 0.05$.
[‡] Significantly different from the low-fat diet with the same dietary lipid as a source; $p < 0.05$.
[†] Significantly different from low-fat control diet group; $p < 0.05$.

Please cite this article in press as: Obara N et al. Possible involvement and the mechanisms of excess *trans*-fatty acid consumption in severe NAFLD in mice. J Hepatol (2010), doi:10.1016/j.jhep.2010.02.029

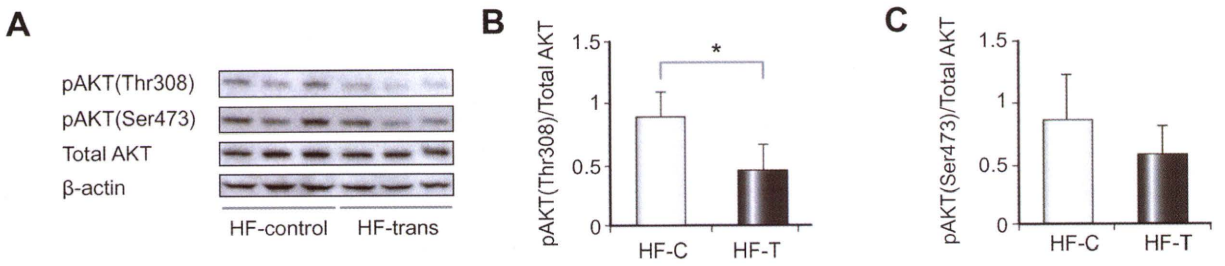

Fig. 3. Effect of excessive TFA consumption of AKT in the high-fat diet-fed mice liver. (A) Representative pictures of phospho-AKT (Thr308 and Ser473), total AKT and β-actin Western blots as well as densitometric analysis of the (B) pAKT(Thr308) or (C) pAKT(Thr473)/total AKT ratio. *$p < 0.05$.

though a few studies have reported that hepatic steatosis [30] and ALT elevation [17] were induced by a TFA-rich diet in mice, the mechanisms remain to be clarified. In agreement with this, the HF-T group showed severe steatosis with a significant transaminase elevation, while HF-C-fed mice only showed moderate steatosis without liver injury, in addition we showed that relatively small amounts of TFA-rich oil intake do not induce severe steatosis and liver injury in the current study. Interestingly, the plasma cholesterol fraction was significantly altered even in the LF-T group in association with the elevation of the total: HDL-cholesterol ratio, a risk factor index of coronary artery disease [22]. The alteration of the plasma cholesterol fraction might be partially explained by changes in the cholesterol metabolism-related gene expressions in the HF-T group, but not in the LF-T group. We could not determine why the cholesterol fraction was altered in the LF-T group, but it might be partially due to the modified membrane fluidity induced by TFA intake [14]. That a relatively small TFA intake could affect the cholesterol fraction but not the liver might be the reason why less attention has been paid to the liver until recently.

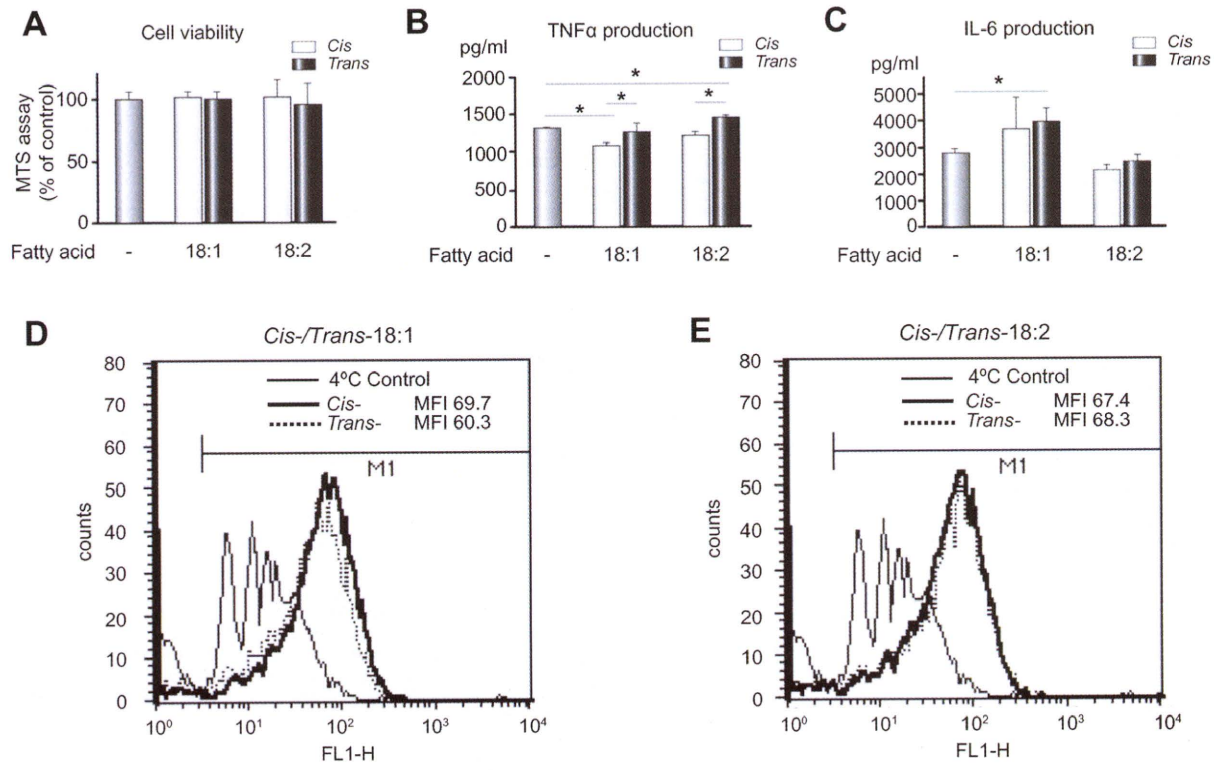

Fig. 4. The impact of *cis-/trans*-fatty acid on the cytokine production and phagocytotic ability of KCs. (A) No fatty acids (200 μM) shows cytotoxicity for primary KCs after 24 h incubation, but (B) increases TNFα production in both C18:1 and C18:2-TFA-containing medium compared to its *cis*-structural isomer. (D) IL-6 production increases in C18:1-containing medium and remains unchanged in C18:2-containing medium, whereas the *cis*- or *trans*-structural difference does affect the results. The influence of the C18:1 (D) and C18:2 (E) *cis-/trans*-fatty acid on the phagocytotic ability of KCs is measured by flow cytometry analysis. MFI: mean fluorescence intensity ($n = 8$ for each group, A–C). *$p < 0.05$.

Please cite this article in press as: Obara N et al. Possible involvement and the mechanisms of excess *trans*-fatty acid consumption in severe NAFLD in mice. J Hepatol (2010), doi:10.1016/j.jhep.2010.02.029

Research Article

One of the noted biochemical changes seen in the HF-T group was the elevation of plasma FFA, almost all of which is derived from adipose tissue and accumulates in the liver as TG in a dose-dependent fashion [7]. The increase of plasma FFA might be due to the TFA incorporation in the adipocyte plasma membrane resulting in decreased membrane fluidity, accompanied by increased adipose tissue insulin resistance as evidenced by increased lipolysis, decreased antilipolysis and decreased glucose uptake in rat adipocytes [14]. In addition, in contrast to TG, the circulating FFAs [21] and accumulation of FFAs in liver [32] are known to exert lipotoxicity to hepatocytes, so the significant increase of the plasma FFA in the HF-T group might affect the pathophysiology. On the other hand, hepatic FFA was higher in HF than LF irrespective of the dietary lipid sources, and it was reported that forced high-fat feeding induced NASH in mice, while usual high-fat intake does not [6]. Hepatic FFA accumulation remained unaltered among healthy, NAFLD and NASH subjects liver [24], so it might not be necessary for the progression to NASH but could be a exacerbating factor in the case of excess fat consumption. Therefore, elevated plasma FFA and accumulated hepatic lipid peroxide [23] would contribute synergistically to the liver injury in this model.

A previous study reported that TFA intake decreased the arachidonic acid level and induced insulin resistance in adipose tissue, probably due to the decreased membrane fluidity [14], and the present study also revealed a decrease of the arachidonic acid level in the liver and lower phosphorylation status of AKT which could reflect the hepatic insulin resistant status in the HF-T group. In addition, a human lipidomic analysis of NAFLD/NASH liver described a decrease of arachidonic acid and unaltered levels of precursor linoleic acid, but the study did not address TFA consumption [24]. Although, the mechanisms of the arachidonic acid decrease and involvement in the insulin resistance and progression to NASH remain to be clarified, these common findings might suggest that TFA intake influences both the liver and adipose tissue in a somewhat similar fashion in NASH patients and people who consume excess TFAs.

Typical pathological findings in human NAFLD/NASH patients such as macrovesicular lipid deposit and inflammation are usually identified around zone 3, though the mice liver showed lipid deposits around zone 1 even in the control lipid-fed group. Microvesicular lipid droplets were remarkable in the HF-T group, so it might be difficult to assess the pathological changes using a human scoring system such as NAS. The pathological differences might be due to a specific problem, since the pediatric NAFLD is known to show histological findings around zone 1 [26], which might be related to the dietary habit of consuming excess TFAs from snacks and first food.

Although the expression of proinflammatory cytokines such as TNFα [30] and IL-1β [17] have been shown to be induced in the mice liver by TFA-rich diets, this was not the case in the current study. However, a previous study reported that, among hypercholesterolemic subjects, the production of TNFα by cultured mononuclear cells was increased by a TFA-rich soy bean margarine diet compared with a natural soybean oil diet [12], and we showed KCs increased TNFα production in TFA-containing medium compared to that of *cis*-structural isomer-containing medium. Accordingly, pathophysiological conditions induced by TFA consumption could be partially due to alterations in the monocyte/macrophage ability in proinflammatory cytokine production and phagocytosis, and KCs in particular may play important roles in the local circumstances.

With regard to the adipokines, the adiponectin levels were not changed between the HF-C and HF-T group, but plasma leptin was significantly increased in the HF-T group. Leptin is an appetite-suppressing and body weight-regulating adipokine, and is even related to liver regeneration and fibrosis [13]; hyperleptinemia might be related directly to the elevation of type1 collagen α1 mRNA expression in the liver.

In terms of the severe steatosis of the model, the lipogenetic genes such as FAS, ACC, SREBP-1 and PPARγ2 were coordinately induced, but PGC-1β was not. PGC-1β is known to be induced in the liver by short term high-fat feeding, to coactivate SREBP-1, but to reduce hepatic fat accumulation. However, since it was not investigated in this study, the decrease of PGC-1β gene expression might be due to long term feeding or any other factors, such as the relatively low carbohydrate diet. It was reported that a TFA-rich diet suppressed the PPARγ gene expression in rat adipose tissue [8], and that lipogenic gene expressions in the liver and the adipose tissue are reciprocal modulations [4], which might reflect the core mechanisms of the heterotopic fat accumulation *in vivo*.

In summary, excess TFA consumption induces significant hepatic steatosis accompanied by augmentation of the hepatic lipogenic gene expressions, FFA influx into the liver, and the hepatic accumulation of lipid peroxide. The hepatic accumulation of TFA and the reduction of the arachidonic acid content were the lipidomic properties in this model. Together with their potential induction of local cytokines by KCs, lipid species including TFA may play a pivotal role in the development of non-alcoholic fatty liver diseases.

Acknowledgements

This study was supported in part from Health and Labour Sciences Research Grants for the Research on Measures for Intractable Diseases (from the Ministry of Health, Labour and Welfare of Japan), from Grant-in-Aid for Scientific Research C (20590755 to KF) from Japanese Society of Promotion of Science (JSPS).

Appendix A. Supplementary data

Supplementary data associated with this article can be found, in the online version, at doi:10.1016/j.jhep.2010.02.029.

References

[1] Babior BM. Oxygen-dependent microbial killing by phagocytes (first of two parts). N Engl J Med 1978;298:659–668.
[2] Browning JD, Szczepaniak LS, Dobbins R, Nuremberg P, Horton JD, Cohen JC, et al. Prevalence of hepatic steatosis in an urban population in the United States: impact of ethnicity. Hepatology 2004;40:1387–1395.
[3] Buettner R, Parhofer KG, Woenckhaus M, Wrede CE, Kunz-Schughart LA, Scholmerich J, et al. Defining high-fat-diet rat models: metabolic and molecular effects of different fat types. J Mol Endocrinol 2006;36:485–501.
[4] Cao H, Gerhold K, Mayers JR, Wiest MM, Watkins SM, Hotamisligil GS. Identification of a lipokine, a lipid hormone linking adipose tissue to systemic metabolism. Cell 2008;134:933–944.
[5] Day CP, James OF. Steatohepatitis: a tale of two "hits"? Gastroenterology 1998;114:842–845.

Please cite this article in press as: Obara N et al. Possible involvement and the mechanisms of excess *trans*-fatty acid consumption in severe NAFLD in mice. J Hepatol (2010), doi:10.1016/j.jhep.2010.02.029

[6] Deng QG, She H, Cheng JH, French SW, Koop DR, Xiong S, et al. Steatohepatitis induced by intragastric overfeeding in mice. Hepatology 2005;42:905–914.
[7] Donnelly KL, Smith CI, Schwarzenberg SJ, Jessurun J, Boldt MD, Parks EJ. Sources of fatty acids stored in liver and secreted via lipoproteins in patients with nonalcoholic fatty liver disease. J Clin Invest 2005;115:1343–1351.
[8] Duque-Guimaraes DE, de Castro J, Martinez-Botas J, Sardinha FL, Ramos MP, Herrera E, et al. Early and prolonged intake of partially hydrogenated fat alters the expression of genes in rat adipose tissue. Nutrition 2009;25:782–789.
[9] Farrell GC, Larter CZ. Nonalcoholic fatty liver disease: from steatosis to cirrhosis. Hepatology 2006;43:S99–S112.
[10] Folch J, Lees M, Sloane Stanley GH. A simple method for the isolation and purification of total lipides from animal tissues. J Biol Chem 1957;226:497–509.
[11] Gonzalez-Periz A, Horrillo R, Ferre N, Gronert K, Dong B, Moran-Salvador E, et al. Obesity-induced insulin resistance and hepatic steatosis are alleviated by omega-3 fatty acids: a role for resolvins and protectins. FASEB J 2009;23:1946–1957.
[12] Han SN, Leka LS, Lichtenstein AH, Ausman LM, Schaefer EJ, Meydani SN. Effect of hydrogenated and saturated, relative to polyunsaturated, fat on immune and inflammatory responses of adults with moderate hypercholesterolemia. J Lipid Res 2002;43:445–452.
[13] Honda H, Ikejima K, Hirose M, Yoshikawa M, Lang T, Enomoto N, et al. Leptin is required for fibrogenic responses induced by thioacetamide in the murine liver. Hepatology 2002;36:12–21.
[14] Ibrahim A, Natrajan S, Ghafoorunissa R. Dietary trans-fatty acids alter adipocyte plasma membrane fatty acid composition and insulin sensitivity in rats. Metabolism 2005;54:240–246.
[15] Kechagias S, Ernersson A, Dahlqvist O, Lundberg P, Lindstrom T, Nystrom FH. Fast-food-based hyper-alimentation can induce rapid and profound elevation of serum alanine aminotransferase in healthy subjects. Gut 2008;57:649–654.
[16] Kleiner DE, Brunt EM, Van Natta M, Behling C, Contos MJ, Cummings OW, et al. Design and validation of a histological scoring system for nonalcoholic fatty liver disease. Hepatology 2005;41:1313–1321.
[17] Koppe SW, Elias M, Moseley RH, Green RM. Trans fat feeding results in higher serum alanine aminotransferase and increased insulin resistance compared with a standard murine high-fat diet. Am J Physiol Gastrointest Liver Physiol 2009;297:G378–G384.
[18] Larter CZ, Yeh MM, Haigh WG, Williams J, Brown S, Bell-Anderson KS, et al. Hepatic free fatty acids accumulate in experimental steatohepatitis: role of adaptive pathways. J Hepatol 2008;48:638–647.
[19] Lin J, Yang R, Tarr PT, Wu PH, Handschin C, Li S, et al. Hyperlipidemic effects of dietary saturated fats mediated through PGC-1beta coactivation of SREBP. Cell 2005;120:261–273.
[20] Lopez-Garcia E, Schulze MB, Meigs JB, Manson JE, Rifai N, Stampfer MJ, et al. Consumption of trans fatty acids is related to plasma biomarkers of inflammation and endothelial dysfunction. J Nutr 2005;135:562–566.
[21] Malhi H, Gores GJ. Molecular mechanisms of lipotoxicity in nonalcoholic fatty liver disease. Semin Liver Dis 2008;28:360–369.
[22] Mensink RP, Zock PL, Kester AD, Katan MB. Effects of dietary fatty acids and carbohydrates on the ratio of serum total to HDL cholesterol and on serum lipids and apolipoproteins: a meta-analysis of 60 controlled trials. Am J Clin Nutr 2003;77:1146–1155.
[23] Milagro FI, Campion J, Martinez JA. Weight gain induced by high-fat feeding involves increased liver oxidative stress. Obesity (Silver Spring) 2006;14:1118–1123.
[24] Puri P, Baillie RA, Wiest MM, Mirshahi F, Choudhury J, Cheung O, et al. A lipidomic analysis of nonalcoholic fatty liver disease. Hepatology 2007;46:1081–1090.
[25] Reid AE. Nonalcoholic steatohepatitis. Gastroenterology 2001;121:710–723.
[26] Schwimmer JB, Behling C, Newbury R, Deutsch R, Nievergelt C, Schork NJ, et al. Histopathology of pediatric nonalcoholic fatty liver disease. Hepatology 2005;42:641–649.
[27] Shimano H, Horton JD, Hammer RE, Shimomura I, Brown MS, Goldstein JL. Overproduction of cholesterol and fatty acids causes massive liver enlargement in transgenic mice expressing truncated SREBP-1a. J Clin Invest 1996;98:1575–1584.
[28] Su GL, Klein RD, Aminlari A, Zhang HY, Steinstraesser L, Alarcon WH, et al. Kupffer cell activation by lipopolysaccharide in rats: role for lipopolysaccharide binding protein and toll-like receptor 4. Hepatology 2000;31:932–936.
[29] Sun Q, Ma J, Campos H, Hankinson SE, Manson JE, Stampfer MJ, et al. A prospective study of trans fatty acids in erythrocytes and risk of coronary heart disease. Circulation 2007;115:1858–1865.
[30] Tetri LH, Basaranoglu M, Brunt EM, Yerian LM, Neuschwander-Tetri BA. Severe NAFLD with hepatic necroinflammatory changes in mice fed trans fats and a high-fructose corn syrup equivalent. Am J Physiol Gastrointest Liver Physiol 2008;295:G987–G995.
[31] Tsuzuki T, Tokuyama Y, Igarashi M, Nakagawa K, Ohsaki Y, Komai M, et al. Alpha-eleostearic acid (9Z11E13E-18:3) is quickly converted to conjugated linoleic acid (9Z11E-18:2) in rats. J Nutr 2004;134:2634–2639.
[32] Yamaguchi K, Yang L, McCall S, Huang J, Yu XX, Pandey SK, et al. Inhibiting triglyceride synthesis improves hepatic steatosis but exacerbates liver damage and fibrosis in obese mice with nonalcoholic steatohepatitis. Hepatology 2007;45:1366–1374.
[33] Zhang YL, Hernandez-Ono A, Siri P, Weisberg S, Conlon D, Graham MJ, et al. Aberrant hepatic expression of PPARgamma2 stimulates hepatic lipogenesis in a mouse model of obesity, insulin resistance, dyslipidemia, and hepatic steatosis. J Biol Chem 2006;281:37603–37615.

Please cite this article in press as: Obara N et al. Possible involvement and the mechanisms of excess *trans*-fatty acid consumption in severe NAFLD in mice. J Hepatol (2010), doi:10.1016/j.jhep.2010.02.029

MAJOR ARTICLE

Hepatitis B Virus Replication Could Enhance Regulatory T Cell Activity by Producing Soluble Heat Shock Protein 60 From Hepatocytes

Yasuteru Kondo,[1] Yoshiyuki Ueno,[1] Koju Kobayashi,[2] Eiji Kakazu,[1] Masaaki Shiina,[1] Jun Inoue,[1] Keiichi Tamai,[1] Yuta Wakui,[1] Yasuhito Tanaka,[5] Masashi Ninomiya,[1] Noriyuki Obara,[1] Koji Fukushima,[1] Motoyasu Ishii,[3] Tomoo Kobayashi,[4] Hirofumi Niitsuma,[1] Satonori Kon,[2] and Tooru Shimosegawa[1]

[1]Division of Gastroenterology, Tohoku University Hospital, [2]School of Health Science, Tohoku University, [3]Department of Gastroenterology, Miyagi Social Insurance Hospital, and [4]Department of Gastroenterology, Tohoku Rosai Hospital, Sendai, and [5]Clinical Molecular Informative Medicine, Nagoya City University, Nagoya, Japan

Background. HBcAg-specific regulatory T (T_{reg}) cells play an important role in the pathogenesis of chronic hepatitis B. Soluble heat shock proteins, especially soluble heat shock protein 60 (sHSP60), could affect the function of T_{reg} cells via Toll-like receptor.

Methods. We analyzed the relationship between soluble heat shock protein production and hepatitis B virus (HBV) replication with both clinical samples from HBeAg-positive patients with chronic hepatitis B ($n = 24$) and HBeAb-positive patients with chronic hepatitis B ($n = 24$) and in vitro HBV-replicating hepatocytes. Thereafter, we examined the biological effects of sHSP60 with isolated T_{reg} cells.

Results. The serum levels of sHSP60 in patients with chronic hepatitis B were statistically significantly higher than those in patients with chronic hepatitis C ($P < .01$), and the levels of sHSP60 were correlated with the HBV DNA levels ($R = 0.532$; $P < .001$) but not with the alanine aminotransferase levels. Moreover, the levels of sHSP60 in HBV-replicating HepG2 cells were statistically significantly higher than those in control HepG2 cells. Preincubation of $CD4^+$ $CD25^+$ cells with recombinant HSP60 (1 ng/mL) statistically significantly increased the frequency of HBcAg-specific interleukin 10–secreting T_{reg} cells. The frequency of $IL7R^-CD4^+CD25^+$ cells, the expression of Toll-like receptor 2, and the suppressive function of T_{reg} cells had declined during entecavir treatment.

Conclusion. The function of HBcAg-specific T_{reg} cells was enhanced by sHSP60 produced from HBV-infected hepatocytes. Entecavir treatment suppressed the frequency and function of T_{reg} cells; this might contribute to the persistence of HBV infection.

Hepatitis B virus (HBV) is a noncytopathic DNA virus that causes chronic hepatitis and hepatocellular carcinoma as well as acute hepatitis and fulminant hepatitis [1]. HBV now affects more than 400 million people worldwide [2], and persistent infection develops in ~5% of adults and 95% of neonates who become infected with HBV.

It has been shown that the cellular immune system, including cytotoxic T lymphocytes, $CD4^+$ T helper 1 cells, and $CD4^+C25^+FoxP3^+$ regulatory T (T_{reg}) cells, plays a central role in the control of viral infection [3–6]. The hyporesponsiveness of HBV-specific T helper 1 cells and the excessive regulatory function of T_{reg} cells in peripheral blood in patients with chronic hepatitis B has been shown elsewhere [7–10]. Lamivudine treatment of chronic hepatitis B has been reported to restore both $CD4^+$ T cells and cytotoxic T lymphocyte hyporesponsiveness following the decrease of serum levels of HBV DNA and HBV-derived Ag [8, 11–13]. In our previous study, we observed that HBcAg-specific interleukin 10 (IL-10)–secreting T_{reg} cells could play an important role in the immunopathogenesis of chronic hepatitis B [9].

Received 14 July 2009; accepted 3 February 2010; electronically published 9 June 2010.

Potential conflicts of interest: none reported.

Financial support: Ministry of Health, Labor, and Welfare of Japan (Health and Labor Sciences Research Grants for the Research on Measures for Intractable Diseases); Ministry of Education, Culture, Sports, Science, and Technology of Japan (grant 21790642 to Y.K.).

Reprints or correspondence: Yoshiyuki Ueno, Division of Gastroenterology, Tohoku University Graduate School of Medicine, Seiryo 1-1, Aobaku, Sendai, 980-8574, Japan (yueno@mail.tains.tohoku.ac.jp).

The Journal of Infectious Diseases 2010;202(2):000–000

0022-1899/2010/20202-00XX$15.00
DOI: 10.1086/653496

Table 1. Clinical Characteristics of Patients with Chronic Hepatitis B or Chronic Hepatitis C Included in This Study

Characteristic	Patients with chronic hepatitis B		Patients with chronic hepatitis C
	HBeAg-positive, HBeAb-negative patients	HBeAg-negative, HBeAb-positive patients	
Age, years	45.16 (12.46)	48.21 (10.23)	48.63 (7.96)
Sex, no. of patients			
Male	12	12	12
Female	12	12	12
ALT level, IU/L	76.91 (39.82)	75.96 (45.90)	76.21 (33.77)
HBV DNA level, log copies/mL	7.83 (0.86)	6.00 (0.81)	NA
Genotype, % of patients			
A	0	4.17	NA
B	12.5	8.33	NA
C	87.5	87.5	NA

NOTE. Data are mean values (standard deviations), unless otherwise indicated. ALT, alanine aminotransferase; HBV, hepatitis B virus; NA, not applicable.

Many research groups have reported the possible induction of anergy by T_{reg} cells, which constitutively express CD25 (the interleukin 2 receptor α chain) in the physiological state [14–16]. In humans, this population of T_{reg} cells, as defined by $CD4^+CD25^+CTLA4^+$ cells, $CD4^+CD25^+FoxP3^+$ cells, or $CD4^+CD25^+IL7R^-$ cells, constitutes 5%–10% of peripheral $CD4^+$ T cells and has a broad repertoire that recognizes various self and nonself antigens. It has been reported that T_{reg} cells have several different mechanisms in suppressing various kinds of immune cells [17, 18]. The important mechanisms are cell to cell contact and secretion of cytokines including IL-10 and transforming growth factor β (TGF-β) [19, 20]. HBcAg derived from HBV might induce T_{reg} cells to escape from immunological pressure, as reported in persistent infection with Epstein-Barr virus, hepatitis C virus (HCV), and human immunodeficiency virus type 1 [21–23]. Some results have indicated that reduction of HBV replication could reduce the frequency and/or function of T_{reg} cells in patients with chronic hepatitis B [4, 5, 8]. However, the key factors that affect HBcAg-specific T_{reg} cells in the replication of HBV remain unclear.

The mammalian 60-kDa heat shock protein is a many-faceted molecule. In addition to serving as a chaperone, heat shock protein 60 (HSP60) is expressed by different types of cells following their exposure to stress or immune responses and is present in the blood during inflammation [24–27]. Recently, HSP60 was reported to enhance the function of $CD4^+CD25^+$ regulatory T cell function via Toll-like receptor 2 (TLR2) signaling [28].

In this study, we investigated the serum level of HSP60 in patients with chronic hepatitis B and the relevance of HBcAg-specific IL-10-secreting T_{reg} cells and HSP60. We report evidence of the production of soluble HSP60 (sHSP60) from HBV-replicating hepatocytes, by use of clinical samples from patients with chronic hepatitis B and an in vitro HBV replication system. In addition, reductions of $CD4^+CD25^+IL7R^-$ T_{reg} cells and TLR2 expression on T_{reg} cells were observed during entecavir therapy. This study could contribute to better understanding of the immunopathogenesis of chronic hepatitis B and the development of immune-based treatment.

MATERIALS AND METHODS

Patients. Forty-eight patients with chronic hepatitis B were enrolled in this study (Table 1). The patients had serum levels of HBV DNA of >5.0 log copies/mL and had elevated alanine aminotransferase (ALT) levels (reference range, <40 IU/L) for >6 months prior to the study. To focus the analysis on the active phase of chronic hepatitis B, we excluded asymptomatic carriers and patients with immune tolerance by age (<30 years old), ALT values (<40 IU/L), and HBV DNA levels (<5.0 log copies/mL). Twenty-four patients were seropositive for HBeAg, and 24 patients were seropositive for anti-HBeAb. None of the patients tested positive for antibodies to hepatitis C virus or had liver disease due to other causes, such as alcohol, drugs, congestive heart failure, and autoimmune disease. Twenty-four patients with chronic hepatitis C and 10 healthy subjects were included as control subjects. Permission for the study was obtained from the Ethics Committee at Tohoku University Graduate School of Medicine (permission no. 2006-194]). Written informed consent was obtained from all the participants enrolled in this study. Participants were monitored for 6 months, and peripheral blood samples were obtained and assessed at 1, 2, 3, and 6 months. At each assessment, patients were evaluated for serum levels of HBV DNA, HBeAg, and anti-HBe, blood chemistry, and hematology. Levels of HBsAg, anti-HBs, total and immunoglobulin anti-HBc, HBeAg, anti-HBe, and anti–

hepatitis C virus were determined by means of commercial enzyme immunoassay kits (Abbott Laboratories). Serum levels of HBV DNA were measured by means of an Amplicor polymerase chain reaction (PCR) assay (lower limit of detection, 2.6 log copies/mL; Roche). High titers of HBV DNA were measured by means of a transcription-mediated amplification-hybridization protection assay (TMA; lower limit of detection, 3.7 log genome equivalents per milliliter). Data were adjusted by means of the following formula: Amplicor value = 0.83 × (TMA value) + 0.67.

Reagents. The following antibodies were used: CD3–allophycocyanin (APC), CD4–peridinin chlorophyll protein complex (PerCP), CD25–fluorescein isothiocyanate (FITC), CD25-phycoerythrin (PE), CD127-PE, Alexa Fluor 488 mouse anti–human CD282 (TLR2), CD284 (Toll-like receptor 4 [TLR4]), and isotype-matched control antibodies purchased from BD Bioscience. Recombinant HBcAg was obtained from Biodesign International. Recombinant HSP60 (rHSP60) was purchased from Stressgen.

Quantification of sHSP60 and soluble heat shock protein 70 (sHSP70) levels. Levels of HSP60 and heat shock protein 70 (HSP70) were quantified by use of HSP60 and HSP70 enzyme-linked immunosorbent assay (ELISA) kits (Stressgen). The serum samples from patients and supernatants from cell cultures were collected at sampling points and stocked at −20°C. The ELISA procedure was performed according to the manufacturer's protocol. First, 100-μL prepared samples were added to wells of anti-HSP60-coated plates. Then the reaction of the anti-HSP60 and horseradish peroxidase conjugate was performed after incubation and washing. Absorbance was measured at 450 nm. The HSP60 sample concentration was calculated by use of a standard curve.

Isolation of peripheral blood mononuclear cells (PBMCs) and T_{reg} cells. PBMCs were isolated from fresh heparinized blood by means of Ficoll-Hypaque density gradient centrifugation. T_{reg} cells were isolated by use of a Dynabeads regulatory $CD4^+CD25^+$ T cell kit (Invitrogen). T_{reg} cells were isolated according to the manufacturer's protocol. In brief, $CD4^+$ cells were isolated from PBMCs by means of negative selection. The remaining cells included the PBMCs depleted of $CD4^+$ cells. Then the $CD4^+CD25^+$ cells were selected positively by use of $CD25^+$ antibody combined with beads. Finally, the beads were detached by means of Detachabead (Invitrogen), because the function of T_{reg} cells might be modified by anti-CD25 antibody.

Coculture of γ-irradiated HBcAg-presenting antigen-presenting cells (APCs) and T_{reg} cells. During the isolation of T_{reg} cells, PBMCs depleted of $CD4^+$ cells could be obtained for use as APCs. PBMCs depleted of $CD4^+$ cells were stimulated at 1×10^6 cells/mL in Roswell Park Memorial Institute 1640 medium containing 10% fetal bovine serum with HBcAg (10 μg/mL) for 12 h at 37°C. Then these γ-irradiated cells were coincubated with 1×10^5 isolated T_{reg} cells that were untreated pretreated with TLR2 and TLR4 neutralizing antibody and rHSP60 (1 ng/mL) (Figures 1*A* and 2).

IL-10 secretion assay. Isolated T_{reg} cells were stimulated with HBcAg-presenting autologous γ-irradiated APCs for 12 h at 37°C. IL-10-secreting cells were stained by adding 10 μL of IL-10-detection antibody (PE-conjugated) together with anti-CD4-PerCP, anti-CD25-FITC, and anti-CD3-APC.

Flow cytometry. PBMCs were stained with CD3-APC, CD4-PerCP, CD25-FITC, and CD127-PE antibodies for 15 min on ice to analyze the frequency of $CD4^+CD25^+IL7R^-$ cells. CD4-PerCP, CD25-PE, and Alexa Fluor 488 mouse anti–human CD282 (TLR2) or CD284 (TLR4) were used for the analysis of TLR2 and TLR4 expression on $CD4^+CD25^+$ cells. Isotype-matched control antibodies were used for adjustment of the fluorescence intensity.

Construction of plasmids. The HBV plasmids was constructed as described elsewhere, with minor modifications [29]. In brief, a serum sample from one of the consecutive patients with fulminant hepatitis B (fulminant hepatitis clone 2), whose serum level of HBV DNA was the highest of the 5 patients, was used to extract total DNA (QIAamp DNA blood mini kit; Qiagen), which was subjected to nested PCR for 2 overlapping fragments; the amplified fragments were nucleotides 1051–3215/1–327 (2492 nucleotides; fragment A) and nucleotides 180–1953 (1774 nucleotides; fragment B). Then the vectors were digested with XbaI, and the XbaI-XbaI site of fragment A-pUC118 was ligated to the XbaI-XbaI site of fragment B-pUC118. Finally, a plasmid containing a 1.3-fold HBV genome (nucleotides 1051–3215/1–1953) was constructed and named pBFH2.

Cell culture and transfection. Human hepatoma HepG2 cells were incubated in Dulbecco modified Eagle medium supplemented with 10% bovine serum at 37°C and 5% carbon dioxide. For the assay of HBV replication, 6-well plates were seeded with 5×10^5 HepG2 or Huh7 cells each. On the next day, 1.5 μg of plasmid DNA were transfected to these cells by use of TransIT LT-1 transfection reagent (Mirus), and the culture supernatant and cells were collected 3 d later. The transfection efficiency was evaluated with a Great EscAPe secreted alkaline phosphatase reporter system 3 (Clontech), in which 10 ng/mL of a reporter plasmid expressing secreted alkaline phosphatase was cotransfected. Experiments were performed at least in triplicate.

Quantification of extracellular HBV DNA, HBsAg, and HBeAg levels. To digest the input plasmid DNA in the culture supernatant, 5 μL of the supernatant was treated with 5 U of DNase I (TaKaRa Bio) at 37°C for 1 h, and the reaction was stopped with edetic acid. Then total DNA was extracted with a QIAamp DNA blood mini kit, and 10 μL of 200-μL DNA solution was subjected to real-time PCR by use of a LightCycler

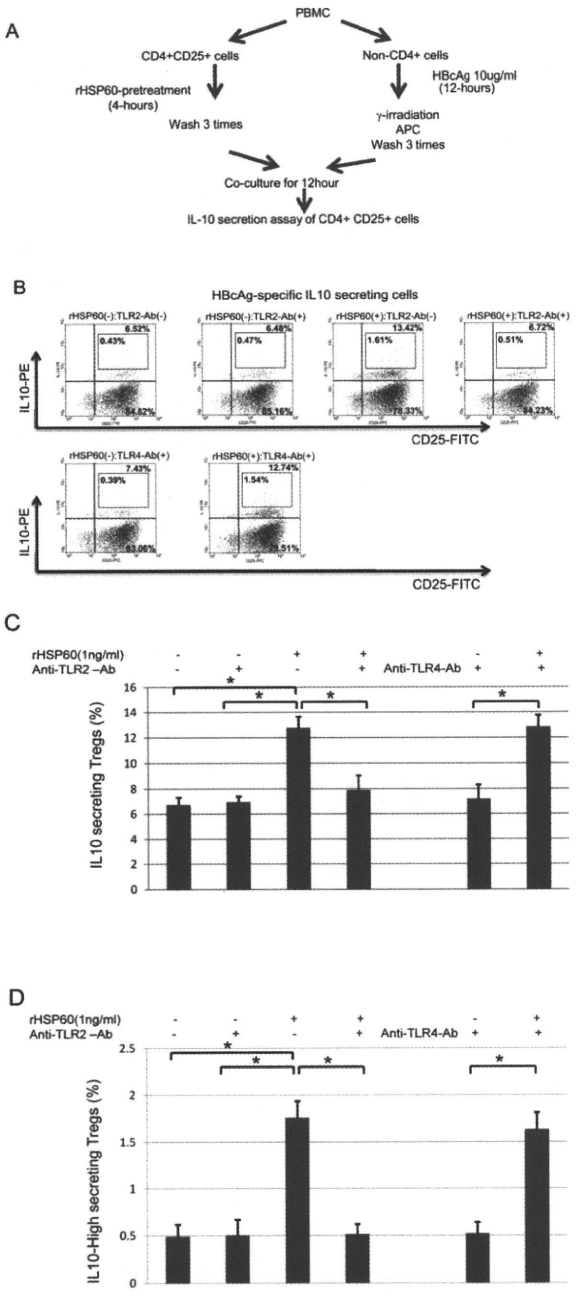

Figure 1. Effects of heat shock protein 60 (HSP60) on HBcAg-specific interleukin 10 (IL-10)–secreting regulatory T (T_{reg}) cells. *A,* Flow chart of the methods. *B,* Representative dot plots of IL-10-secreting cells in the $CD4^+CD25^+$ cells. The mixed cells (antigen-presenting cells [APCs; $CD4^-$] and isolated $CD4^+CD25^+$ cells) were stained with anti-CD4–peridinin chlorophyll protein complex (PerCP), anti-CD25–fluorescein isothiocyanate (FITC), and anti-IL-10-phycoerythrin (PE). The numbers in each top right quadrant indicate the frequencies of $CD25^+$ IL-10-secreting cells among the $CD4^+$ cells. The numbers in each bottom right quadrant indicate the frequencies of $CD4^+CD25^+IL\text{-}10^-$ cells among the $CD4^+$ cells. The numbers in each box in the top right quadrant indicate the frequencies of $CD25^+$ IL-10-secreting cells among the $CD4^+$ cells. *C,* Representative results for a sample from 1 patient with chronic hepatitis B (samples were obtained from 3 patients with chronic hepatitis B; this experiment was repeated 3 times). Bars indicate the percentage of IL-10-secreting cells among the $CD4^+$ cells with various kinds of pretreatment. *D,* Percentage of high–IL-10-secreting cells among the $CD4^+$ cells. Error bars indicate the standard deviation of 3 independent experiments with a sample from 1 patient with chronic hepatitis B. Three independent experiments yielded similar results to those shown in panels *C* and *D*. $^*P < .05$.

This figure is available in its entirety in the online version of the *Journal of Infectious Diseases*.

Figure 2. Effect of recombinant heat shock protein 60 (rHSP60) on the interleukin 10 (IL-10)–secreting activity of $CD4^+CD25^+$ cells.

system (Roche). ELISA kits were used to assay HBsAg (Hope Laboratories) and HBeAg (BioChain Institute) in 50 μL of the culture supernatant.

Sequence analysis of HBV DNA. The presence of HBV DNA in the serum samples was determined by means of PCR, as described elsewhere [30]. Nucleic acids were extracted from 100 mL of serum and subjected to nested PCR for the S gene. The amplification product of the first-round PCR was 461 bp, and that of the second-round PCR was 437 bp. The amplification products were sequenced directly on both strands by use of the BigDye Terminator Cycle Sequencing Ready reaction kit on an ABI Prism 3100 genetic analyzer (Applied Biosystems).

Carboxyfluorescein succinimidyl ester (CFSE) staining and suppression assay. The suppressive activity of regulatory T cells was analyzed by use of a CellTrace CFSE cell proliferation kit (Molecular Probes). Staining methods were followed according to the manufacturer's protocol. Briefly, the collected $CD4^+CD25^-$ cells were washed and resuspended in prewarmed phosphate-buffered saline with 0.1% bovine serum albumin at a final concentration of 3×10^5 cells/mL. CFSE solution (5 μm) was added and incubated at 37°C for 10 min. Stained cells were washed 3 times and incubated with unstained $CD4^+CD25^+$ T_{reg} cells and CD3CD28-coated stimulation beads (T cell expander) for an additional 3 d. The cells were analyzed by means flow cytometry with 488-nm excitation and emission filters.

Statistics. The data in Figures 3, 4, 1*C*, 1*D*, and 5 were analyzed by use of the independent *t* test. Statistical correlation analysis of the data in Figure 6 was performed by use of the Kendall τ_b test. The data in Figure 7 were analyzed by use of the Wilcoxon rank sum test. All of the statistical analyses were performed with SPSS software (version 10.0; SPSS). Results for which $P < .05$ were considered to be statistically significant.

RESULTS

Levels of sHSP60 and sHSP70 in samples from HBeAg-positive patients with chronic hepatitis B, HBeAg-negative patients with chronic hepatitis B, and control patients with chronic hepatitis C. The patients' characteristics, including age, sex, and ALT level, were matched among the different patient groups because the levels of sHSP60 and sHSP70 might be influenced by these factors (Table 1). The mean (± standard deviation [SD]) serum level of sHSP60 was 5.77 ± 1.19 ng/mL in HBeAg-positive patients with chronic hepatitis B, 4.12 ± 1.37 ng/mL in HBeAg-negative patients with chronic hepatitis B, 2.11 ± 0.96 ng/mL in patients with chronic hepatitis C, and 0.54 ± 0.46 ng/mL in healthy subjects. The levels of sHSP60 in patients with chronic hepatitis B (HBeAg-positive and HBeAg-negative) were statistically significantly higher than those in patients with chronic hepatitis C (Figure 3). On the other hand, the mean (± SD) serum level of sHSP70 was 7.89 ± 3.51 ng/mL in HBeAg-positive patients with chronic hepatitis B, 7.73 ± 3.71 ng/mL in HBeAg-negative patients with chronic hepatitis B, 8.09 ± 3.64 ng/mL in patients with chronic hepatitis C, and 3.54 ± 0.46 ng/mL in healthy subjects. There were no statistically significant differences in the level of sHSP70 between the chronic hepatitis B and chronic hepatitis C patient groups (Figure 3). Then we examined the correlations between the HSP60, HSP70, and HBV DNA or ALT levels. The levels of sHSP60 were correlated with the HBV DNA levels ($r = 0.532$; $P < .001$) but not with the ALT levels ($r = 0.101$; $P = .315$) (Figures 6*A* and 6*B*). On the other hand, the levels of sHSP70 were correlated with the ALT levels ($r = 0.520$; $P < .001$) but not with the HBV DNA levels ($r = 0.076$; $P < .449$) (Figure 6*C* and 6*D*).

HBV replication could directly induce sHSP60 production in vitro. Two kinds of plasmids carrying a 1.3-fold HBV genome that could replicate in HepG2 cells were used to analyze whether HBV replication could affect the production of sHSP60 in culture medium. The transfection efficiency was almost the

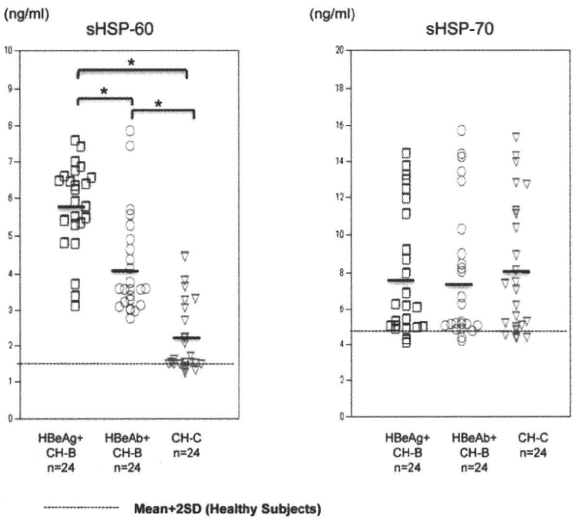

Figure 3. Quantification of serum levels of heat shock protein 60 (HSP60) and heat shock protein 70 (HSP70) in HBeAg-positive patients with chronic hepatitis B (CH-B), HBeAb-positive patients with CH-B, and patients with chronic hepatitis C (CH-C). Serum levels of HSP60 and HSP70 were quantified by means of enzyme-linked immunosorbent assay. The bar represents the means of the levels of HSP60 and HSP70. Dotted lines indicate the mean value plus 2 times the standard deviation (SD) of the levels of healthy subjects.

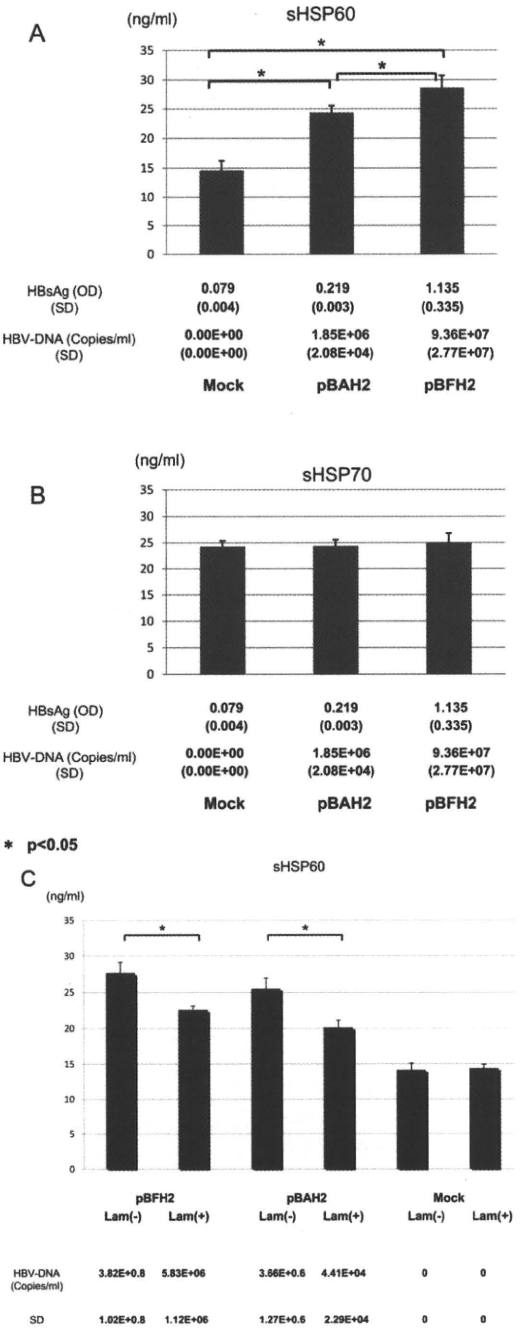

Figure 4. Direct effect of hepatitis B virus (HBV) on the production of heat shock protein 60 (HSP60) and heat shock protein 70 (HSP70). Two kinds of plasmid (pBAH2 and pBFH2) carrying a 1.3-fold HBV genome that could replicate in HepG2 cells and a mock plasmid were used to analyze whether HBV replication affects the production of soluble HSP60 (sHSP60) in culture medium. The levels of sHSP60 and soluble HSP70 (sHSP70) were compared among the 3 plasmid groups. Bars indicate the levels of HSP60 (*A*) and HSP70 (*B*). The HBsAg and HBV DNA levels and standard deviations (SDs) are included below the bar graphs. *C*, Levels of sHSP60 in cells with and those in cells without lamivudine treatment. The cells were treated with lamivudine (Lam; 0.5 μmol/L) for 72 h. Three independent experiments were performed.

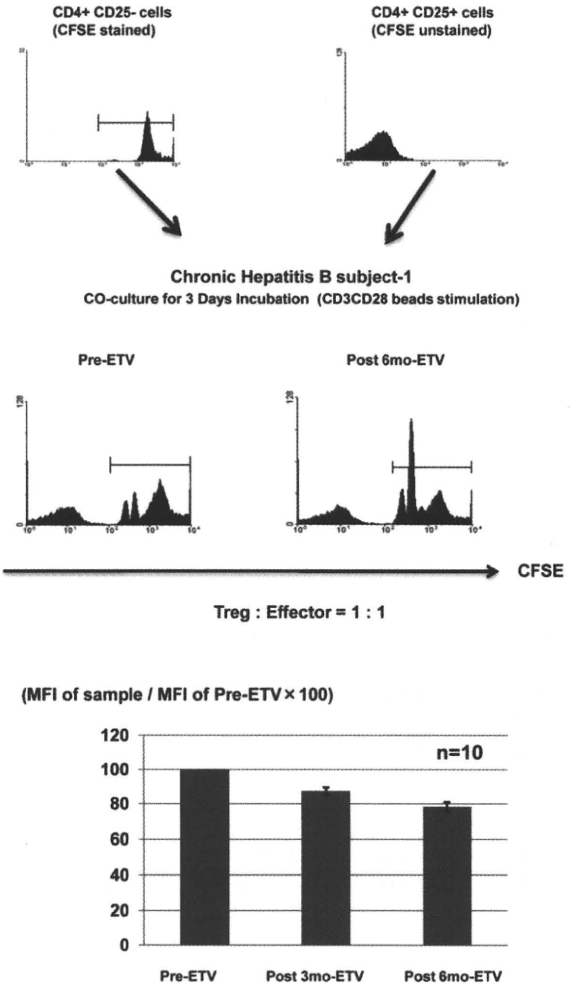

Figure 5. Suppression assay of regulatory T (T_{reg}) cells. The suppressive activity of T_{reg} cells was analyzed by means of coincubation of unstained isolated T_{reg} cells and autologous $CD4^+CD25^-$ cells with carboxyfluorescein succinimidyl ester (CFSE) staining. *A,* Representative histogram of CFSE-stained $CD4^+CD25^-$ effector cells and unstained $CD4^+CD25^+$ T_{reg} cells. *B,* Various levels of cell division in $CD4^+CD25^-$ effector cells observed 3 d after coincubation with CD3CD28-coated beads. *C,* Mean fluorescence intensity (MFI) of CFSE staining of $CD4^+CD25^-$ cells before treatment, 3 months after the start of entecavir (ETV) treatment, and 6 months after the start of entecavir treatment. The bars show the MFI of the samples divided by the MFI of the pretreatment samples ×100. The error bars indicate the standard deviations of the data.

same among the different plasmids (data not shown). The mean (± SD) HBV DNA levels of pBAH2 and pBFH2 were $1.85 \times 10^6 \pm 2.08 \times 10^4$ and $9.36 \times 10^7 \pm 2.77 \times 10^7$ copies/mL, respectively. The levels of sHSP60 in the supernatant of the pBAH2- and pBFH2-transfected HepG2 cells were statistically significantly higher than that of the mock-transfected HepG2 cells ($P < .05$) (Figure 4*A*). However, the levels of sHSP70 in the supernatant of the pBAH2- and pBFH2-transfected HepG2 cells were comparable with that of the mock-transfected HepG2 cells (Figure 4*B*). The addition of HBV-derived antigen in the culture supernatant could not increase the level of sHSP60 (data not shown). We performed the experiment on the suppression of HBV replication by nucleoside analogues in vitro. The suppression of HBV replication could statistically significantly reduce the production of sHSP60 (Figure 4*C*). These data indicate that HBV replication could increase the level of sHSP60 in the supernatant of the hepatocyte culture.

The effect of HSP60 on the HBcAg-specific IL-10-secreting T_{reg} cells. Previously, we found that HBcAg-specific IL-10-secreting cells could play an important role in the hyporesponsiveness of T cells in patients with chronic hepatitis B [9]. The effects of HSP60 on HBcAg-specific IL-10-secreting T_{reg} cells were analyzed. The appropriate dose of rHSP60 pretreatment was determined by use of PBMCs from healthy subjects (Figure 2). Pretreatment with rHSP60 could increase the frequency of HBcAg-specific IL-10-secreting cells statistically significantly ($P < .01$) and enhance the function of IL-10 secretion of HBcAg-specific T_{reg} cells, because the frequencies of high-intensity cells with IL-10 staining in HSP60 pretreatment T_{reg} cells were statistically significantly higher than those of control groups (Figure 1*D*). Moreover, these effects were completely blocked by neutralizing TLR2 antibody but not by TLR4 antibody. These data indicate that HSP60 might enhance the susceptibility and function of IL-10 secretion of HBcAg-specific T_{reg} cells.

Sequential analysis of clinical samples collected during entecavir therapy. Ten patients were selected for sequential analysis during entecavir therapy. The titers of HBV DNA and the ALT level rapidly decreased during entecavir therapy (Figures 7*A* and 7*B*). The serum levels of HSP60 had statistically significantly decreased at 3 months and at 6 months after the start of entecavir therapy. The frequency of T_{reg} cells and the expression level of TLR2 during entecavir treatment were quantified sequentially for up to 6 months during treatment by means of flow cytometry analysis. The frequency of $CD4^+CD25^+$ cells decreased, although not statistically significantly. On the other hand, the frequency of $CD4^+CD25^+IL7R^-$ cells (subpopulation of $CD4^+CD25^+$ cells) had statistically significantly decreased at 3 months and at 6 months after the start of entecavir therapy. The reason for the discrepancy could be that $CD4^+CD25^+$ cells included not only T_{reg} cells but also activated $CD4^+$ effector cells. Previously, some research groups had found that $CD4^+CD25^+FoxP3^+$ cells are almost the same as $CD4^+CD25^+IL7R^-$ cells. Therefore, our data indicate that entecavir therapy could reduce the frequency of T_{reg} cells. We also investigated the frequency of $CD4^+CD25^+FoxP3^+$ cells during lamivudine therapy (Figure 8). The frequency of

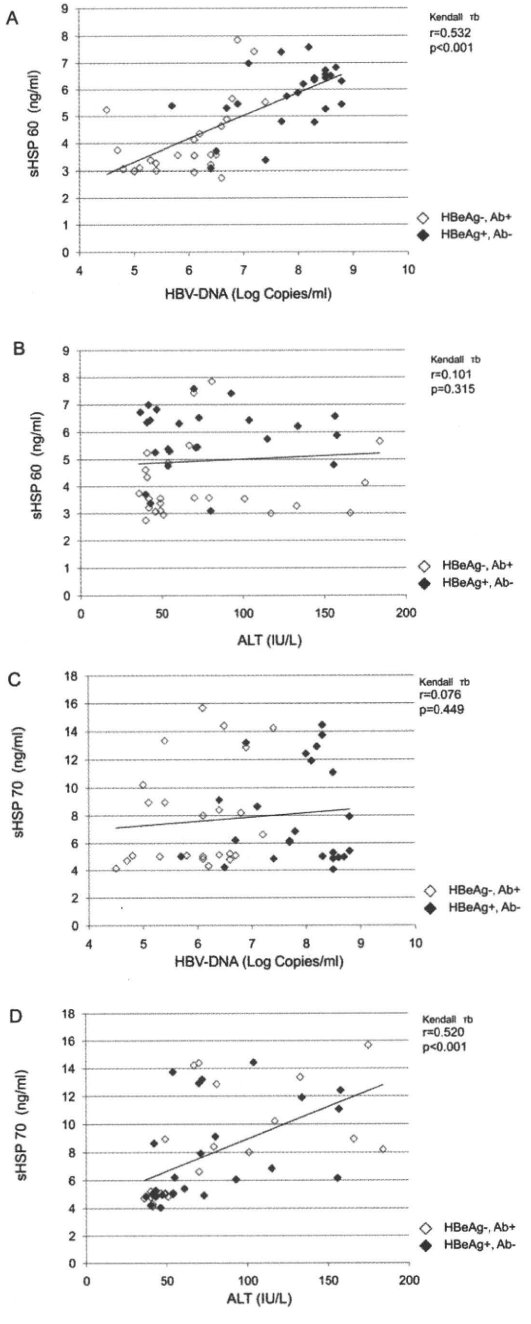

Figure 6. Analysis of the correlations between levels of heat shock proteins (HSPs), hepatitis B virus (HBV) DNA, and alanine aminotransferase (ALT). Open symbols indicate the values in samples from HBeAg-negative, HBeAb-positive patients. Filled symbols indicate the values in samples from HBeAg-positive, HBeAb-negative patients. The statistical analysis was performed by use of nonparametric Kendall τ_b methods. An approximately straight line is included in each graph. *A,* Correlation between heat shock protein 60 (HSP60) level and HBV DNA level. *B,* Correlation between HSP60 level and ALT level. *C,* Correlation between heat shock protein 70 (HSP70) level and HBV DNA level. *D,* Correlation between HSP70 level and ALT level.

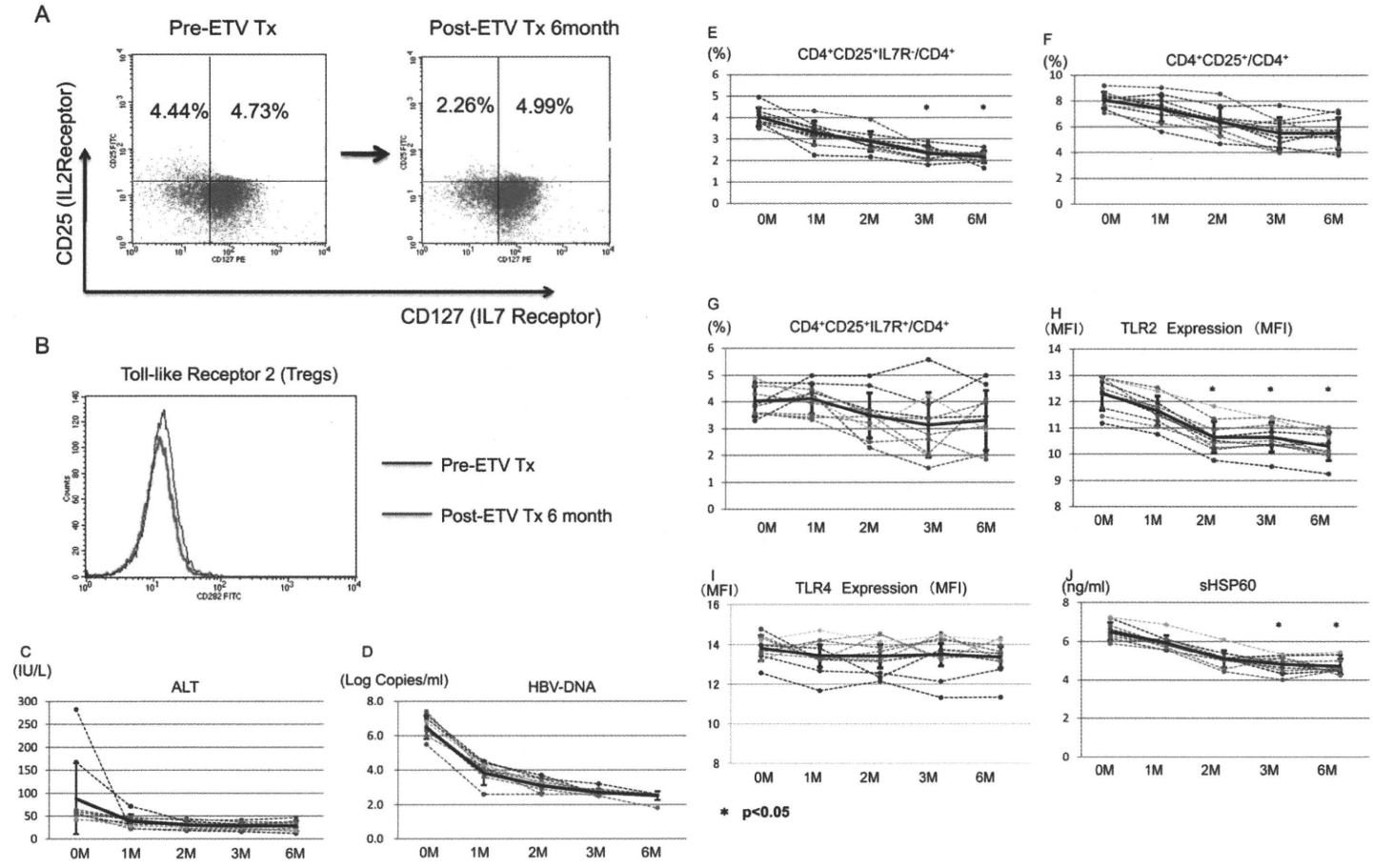

Figure 7. Sequential analysis of primary lymphocytes and soluble heat shock protein 60 (sHSP60) during entecavir (ETV) therapy. *A,* Representative dot plots of the $CD4^+CD25^+IL7R^-$ cells before treatment and 6 months after the start of treatment. Peripheral blood mononuclear cells were stained with anti-CD3, anti-CD4, anti-CD25, and anti–IL7R (CD127). The phenotypes of the $CD4^+$ cells were determined as follows: $CD4^+CD25^+IL7R^-$ cells were identified as regulatory cells and $CD4^+CD25^+IL7R^+$ cells were identified as activated $CD4^+$ cells. *B,* Representative histogram of Toll-like receptor 2 (TLR2) surface expression on $CD4^+CD25^+$ regulatory T (T_{reg}) cells before treatment and 6 months after the start of treatment. *C* and *D,* Serum levels of alanine aminotransferase (ALT) and hepatitis B virus (HBV) DNA during ETV treatment. Solid black lines and error bars indicate the mean values and standard deviations, respectively. *E–G,* Frequencies of $CD4^+CD25^+IL7R^-$cells, $CD4^+CD25^+$ cells, and $CD4^+CD25^+IL7R^+$ cells among $CD4^+$ cells during ETV treatment, respectively. *H* and *I,* Mean fluorescence intensity (MFI) of TLR2 and Toll-like receptor 4 (TLR4) expression on $CD4^+CD25^+$ cells during ETV treatment. *J,* Serum levels of sHSP60 during ETV treatment. $^*P < .01$ for comparison between pretreatment levels and posttreatment levels.

This figure is available in its entirety in the online version of the *Journal of Infectious Diseases*.

Figure 8. Frequency of $CD4^+CD25^+FoxP3^+$ cells.

$CD4^+CD25^+FoxP3^+$ cells was also decreased during lamivudine therapy. Moreover, the expression level of TLR2 on $CD4^+CD25^+$ cells gradually declined during entecavir therapy (Figure 7*G*).

Suppressive activity of T_{reg} cells. The suppressive activity of T_{reg} cells was analyzed by means of coincubation of unstained isolated T_{reg} cells and autologous $CD4^+CD25^-$ cells with CFSE staining. Ex vivo peripheral blood samples from 10 selected patients were analyzed before treatment, 3 months after the start of treatment, and 6 months after the start of treatment. The mean fluorescence intensity of the CFSE staining of the $CD4^+CD25^-$ cells was statistically significantly decreased at 6 months after the start of treatment ($P < .05$). These data indicate that the suppressive activity of T_{reg} cells was gradually decreased during entecavir treatment.

DISCUSSION

In this study, we have demonstrated that the levels of sHSP60 in patients with chronic hepatitis B were statistically significantly higher than those in patients with chronic hepatitis C. Moreover, the levels of sHSP60 were correlated with the HBV DNA levels but not with the ALT levels. On the other hand, the levels of sHSP70 were correlated with the ALT levels but not with the HBV DNA levels. This discrepancy in the correlation might be due to differences in the mechanism of heat shock protein production or secretion. The release of such heat shock proteins from cells is triggered by physical trauma and behavioral stress as well as by exposure to immunological danger signals [31, 32]. Stress protein release occurs both through physiological secretion mechanisms and during cell death by necrosis [33, 34]. HSP60 might be induced by the stress of HBV replication, because the levels of HSP60 were clearly correlated with the HBV DNA levels. On the other hand, HSP70 secretion might also be caused by cell death, because the levels of sHSP70 were correlated with the ALT levels. However, we should wait for more detailed studies about the HBV-specific induction of HSP60 to confirm this correlation. Extracellular stress proteins of the heat shock protein and glucose-regulated stress protein families, including HSP60, have powerful effects on the immune response [35]. Moreover, various kinds of immune cells such as macrophages, dendritic cells, $CD4^+$effector T cells, and T_{reg} cells are affected by heat shock proteins [28, 35]. Most recently, Cohen-Sfady et al [36] reported that HSP60 enhanced the activity of IL-10 secretion from B cells. This effect could support our findings of the immune-suppressive effect of HSP60. However, we can not draw conclusions about the whole effects of immune responses because the various kinds of immune cells might affect each other by means of cytokines, chemokines, stress-related proteins, and direct binding.

In this study, we focused on the effect of HSP60 on T_{reg} cell function by isolating T_{reg} cells, because many research groups had reported that the function and frequency of T_{reg} cells might be related to HBV replication. T_{reg} cells play an important role in the immune-hyporesponsiveness of patients with chronic hepatitis B. Previously, we demonstrated that the polarization of $CD4^+$ T cells was suppressed when the cells were stimulated with HBcAg in patients with chronic hepatitis B. T_{reg} cells are important cells in the suppression of the T helper 1 cell response by HBcAg, as demonstrated by the increased population of IL-10-secreting $CD4^+CD25^+$ cells. This indicates the presence of an inducible T_{reg} cell population, which is specific for HBcAg and produces IL-10, as well as a natural T_{reg} cell population in patients with chronic hepatitis B. Pretreatment with rHSP60 increased the frequency of HBcAg-specific IL-10-secreting $CD4^+CD25^+$ cells and enhanced the IL-10-secreting activity. These results indicate that pretreatment with rHSP60 might enhance the susceptibility of the HBcAg response and the function of IL-10 production by T_{reg} cells. These data might not imply that there was an expansion of HBcAg-specific T_{reg} cells as a result of the rHSP60 pretreatment, because the incubation phase was for only 16 h (4 h of pretreatment with rHSP60 plus 12 h of coincubation with HBcAg-presenting APCs). However, there is a possibility that continuous exposure to sHSP60 might induce an expansion of T_{reg} cells by enhancing the sensitivity of the expansion signal.

In this study, we found that the effect of HSP60 could be blocked by TLR2 neutralizing antibody but not by TLR4 neutralizing antibody. These data indicate that the effect of HSP60 could depend on TLR2. During entecavir therapy, not only the frequency of T_{reg} cells but also the serum levels of HSP60 and surface expression of TLR2 on T_{reg} cells gradually decreased. Therefore, we performed the suppression assay to detect the activity of T_{reg} cells by use of ex vivo isolated T_{reg} cells. The results of this suppression assay indicate that the reduction of the HBV DNA level could suppress the excessive activity of T_{reg} cells. In our previous study, the frequency and the function of HBV-specific cytotoxic T lymphocytes were partially recovered after therapy with nucleoside or nucleotide analogues [11]. The results clearly indicate that this restoration might be due to not only the reduction of HBV antigens but also the reduction of the frequency and function of T_{reg} cells.

On the basis of genomic analysis, 8 genotypes (A–H) of HBV have been defined, among which genotypes A, B, and especially C are prevalent in Japan [37–40]. Previous studies suggested that the clinical outcome of chronic hepatitis B was more severe in patients infected with genotype C, compared with those infected with genotype B [38, 39]. In this study, most of the

samples had HBV genotype C because of the high frequency of HBV genotype C infection in Japan. However, the expression levels of HSP60 were different among samples with the various genotypes in preliminary in vitro studies (data not shown). In addition, the expression patterns of chemokines in HBV-replicating Huh7 cells are apparently different among the various genotypes (Y. Kondo et al, unpublished data, May 2009). However, during entecavir treatment, the level of sHSP60 production in patients with genotype Bj HBV infection was quite similar to that in patients with genotype C HBV infection. We could not determine the relevance of the HBV genotypes and sHSP60 production levels because of the small numbers of genotype Bj–infected patients in this study.

In conclusion, we found that HSP60 was produced by HBV-replicating hepatocytes and determined the relevance of sHSP60 to T_{reg} cells functions, especially for IL-10-secreting activity. The understanding of the immunopathogensis of chronic hepatitis B could contribute to the development of novel kinds of immune therapy. Combination therapy with nucleoside or nucleotide analogues should be a reasonable method, because the suppression of HBV replication could reduce the excessive immune tolerance induced by T_{reg} cells.

References

1. Tiollais P, Pourcel C, Dejean A. The hepatitis B virus. Nature **1985**; 317:489–495.
2. Lai CL, Ratziu V, Yuen MF, Poynard T. Viral hepatitis B. Lancet **2003**; 362:2089–2094.
3. Kagi D, Ledermann B, Burki K, Zinkernagel RM, Hengartner H. Molecular mechanisms of lymphocyte-mediated cytotoxicity and their role in immunological protection and pathogenesis in vivo. Annu Rev Immunol **1996**; 14:207–232.
4. Peng G, Li S, Wu W, Sun Z, Chen Y, Chen Z. Circulating CD4+ CD25+ regulatory T cells correlate with chronic hepatitis B infection. Immunology **2008**; 123:57–65.
5. Barboza L, Salmen S, Goncalves L, et al. Antigen-induced regulatory T cells in HBV chronically infected patients. Virology **2007**; 368:41–49.
6. Kondo Y, Ueno Y, Shimosegawa T. Immunopathogenesis of hepatitis B persistent infection: implications for immunotherapeutic strategies. Clin J Gastroenterol **2009**; 2:71–79.
7. Xu D, Fu J, Jin L, et al. Circulating and liver resident CD4+CD25+ regulatory T cells actively influence the antiviral immune response and disease progression in patients with hepatitis B. J Immunol **2006**; 177: 739–747.
8. Manigold T, Racanelli V. T-cell regulation by CD4 regulatory T cells during hepatitis B and C virus infections: facts and controversies. Lancet Infect Dis **2007**; 7:804–813.
9. Kondo Y, Kobayashi K, Ueno Y, et al. Mechanism of T cell hyporesponsiveness to HBcAg is associated with regulatory T cells in chronic hepatitis B. World J Gastroenterol **2006**; 12:4310–4317.
10. Kondo Y, Kobayashi K, Asabe S, et al. Vigorous response of cytotoxic T lymphocytes associated with systemic activation of CD8 T lymphocytes in fulminant hepatitis B. Liver Int **2004**; 24:561–567.
11. Kondo Y, Asabe S, Kobayashi K, et al. Recovery of functional cytotoxic T lymphocytes during lamivudine therapy by acquiring multi-specificity. J Med Virol **2004**; 74:425–433.
12. Chisari FV, Ferrari C. Hepatitis B virus immunopathogenesis. Annu Rev Immunol **1995**; 13:29–60.
13. Reignat S, Webster GJ, Brown D, et al. Escaping high viral load exhaustion: CD8 cells with altered tetramer binding in chronic hepatitis B virus infection. J Exp Med **2002**; 195:1089–1101.
14. Suri-Payer E, Amar AZ, Thornton AM, Shevach EM. CD4+CD25+ T cells inhibit both the induction and effector function of autoreactive T cells and represent a unique lineage of immunoregulatory cells. J Immunol **1998**; 160:1212–1218.
15. Chen W, Jin W, Hardegen N, et al. Conversion of peripheral CD4+CD25− naive T cells to CD4+CD25+ regulatory T cells by TGF-beta induction of transcription factor Foxp3. J Exp Med **2003**; 198:1875–1886.
16. Hori S, Nomura T, Sakaguchi S. Control of regulatory T cell development by the transcription factor Foxp3. Science **2003**; 299:1057–1061.
17. Suvas S, Kumaraguru U, Pack CD, Lee S, Rouse BT. CD4+CD25+ T cells regulate virus-specific primary and memory CD8+ T cell responses. J Exp Med **2003**; 198:889–901.
18. Nakamura K, Kitani A, Fuss I, et al. TGF-beta 1 plays an important role in the mechanism of CD4+CD25+ regulatory T cell activity in both humans and mice. J Immunol **2004**; 172:834–842.
19. Zheng SG, Wang JH, Gray JD, Soucier H, Horwitz DA. Natural and induced CD4+CD25+ cells educate CD4+CD25− cells to develop suppressive activity: the role of IL-2, TGF-beta, and IL-10. J Immunol **2004**; 172:5213–5221.
20. Sundstedt A, O'Neill EJ, Nicolson KS, Wraith DC. Role for IL-10 in suppression mediated by peptide-induced regulatory T cells in vivo. J Immunol **2003**; 170:1240–1248.
21. Ulsenheimer A, Gerlach JT, Gruener NH, et al. Detection of functionally altered hepatitis C virus-specific CD4 T cells in acute and chronic hepatitis C. Hepatology **2003**; 37:1189–1198.
22. Marshall NA, Vickers MA, Barker RN. Regulatory T cells secreting IL-10 dominate the immune response to EBV latent membrane protein 1. J Immunol **2003**; 170:6183–6189.
23. Beilharz MW, Sammels LM, Paun A, et al. Timed ablation of regulatory CD4+ T cells can prevent murine AIDS progression. J Immunol **2004**; 172:4917–4925.
24. Wallin RP, Lundqvist A, More SH, von Bonin A, Kiessling R, Ljunggren HG. Heat-shock proteins as activators of the innate immune system. Trends Immunol **2002**; 23:130–135.
25. Raz I, Elias D, Avron A, Tamir M, Metzger M, Cohen IR. Beta-cell function in new-onset type 1 diabetes and immunomodulation with a heat-shock protein peptide (DiaPep277): a randomised, double-blind, phase II trial. Lancet **2001**; 358:1749–1753.
26. Hu W, Hasan A, Wilson A, et al. Experimental mucosal induction of uveitis with the 60-kDa heat shock protein-derived peptide 336–351. Eur J Immunol **1998**; 28:2444–2455.
27. Mor F, Cohen IR. T cells in the lesion of experimental autoimmune encephalomyelitis: enrichment for reactivities to myelin basic protein and to heat shock proteins. J Clin Invest **1992**; 90:2447–2455.
28. Zanin-Zhorov A, Cahalon L, Tal G, Margalit R, Lider O, Cohen IR. Heat shock protein 60 enhances CD4+ CD25+ regulatory T cell function via innate TLR2 signaling. J Clin Invest **2006**; 116:2022–2032.
29. Sugiyama M, Tanaka Y, Kato T, et al. Influence of hepatitis B virus genotypes on the intra- and extracellular expression of viral DNA and antigens. Hepatology **2006**; 44:915–924.
30. Inoue J, Takahashi M, Nishizawa T, et al. High prevalence of hepatitis delta virus infection detectable by enzyme immunoassay among apparently healthy individuals in Mongolia. J Med Virol **2005**; 76:333–340.
31. Lindquist S, Craig EA. The heat-shock proteins. Annu Rev Genet **1988**; 22:631–677.
32. Ellis RJ. The molecular chaperone concept. Semin Cell Biol **1990**; 1: 1–9.
33. Hightower LE, Guidon PT Jr. Selective release from cultured mammalian cells of heat-shock (stress) proteins that resemble glia-axon transfer proteins. J Cell Physiol **1989**; 138:257–266.
34. Mambula SS, Calderwood SK. Heat shock protein 70 is secreted from

tumor cells by a nonclassical pathway involving lysosomal endosomes. J Immunol **2006**; 177:7849–7857.
35. Calderwood SK, Mambula SS, Gray PJ Jr, Theriault JR. Extracellular heat shock proteins in cell signaling. FEBS Lett **2007**; 581:3689–3694.
36. Cohen-Sfady M, Pevsner-Fischer M, Margalit R, Cohen IR. Heat shock protein 60, via MyD88 innate signaling, protects B cells from apoptosis, spontaneous and induced. J Immunol **2009**; 183:890–896.
37. Mahmood S, Niiyama G, Kamei A, et al. Influence of viral load and genotype in the progression of hepatitis B-associated liver cirrhosis to hepatocellular carcinoma. Liver Int **2005**; 25:220–225.
38. Akuta N, Suzuki F, Kobayashi M, et al. Virological and biochemical relapse after discontinuation of lamivudine monotherapy for chronic hepatitis B in Japan: comparison with breakthrough hepatitis during long-term treatment. Intervirology **2005**; 48:174–182.
39. Kobayashi M, Suzuki F, Akuta N, et al. Response to long-term lamivudine treatment in patients infected with hepatitis B virus genotypes A, B, and C. J Med Virol **2006**; 78:1276–1283.
40. Tanaka Y, Mizokami M. Genetic diversity of hepatitis B virus as an important factor associated with differences in clinical outcomes. J Infect Dis **2007**; 195:1–4.